Building Simulation

Seventh International IBPSA Conference
Rio de Janeiro, Brazil
August 13-15, 2001

A STUDY ON GENERATING SYSTEM OF THERMAL IMAGES FOR EVALUATION OF RADIATION ENVIRONMENT OF GLASS ENCLOSED SPACE

Hisaya ISHINO[1], Kimiko KOHRI[2] and Masayuki ICHINOSE[3]

[1] Prof., Graduate School of Eng., Tokyo Metropolitan Univ., Dr.Eng.
[2] Prof., Graduate School of Eng., Utsunomiya Univ., Dr.Eng.
[3] Graduate School of Eng., Tokyo Metropolitan Univ., M.Eng.
Tokyo 192-0397, Japan
masayuki@ecomp.metro-u.ac.jp

ABSTRACT

A method for calculating radiant temperature of thermal images is presented. These thermal images include image-generating system of measured thermal images (such as infrared images). Radiant temperature is described from information of luminance distribution, with shape of the human body taken into account. A shading calculation model used in generating computer graphics is applied to thermal radiation calculation for reproducing anisotropic diffuse properties detected from measured infrared images of a glass surface. The effect of surface properties and sensor shape on radiant temperature is studied by way of simulation.

INTRODUCTION

The significance of radiant environment is recognized in the design of the thermal environment of an atrium. An evaluation method (using measured infrared images) of radiant effect from each surface in atria is proposed. The present study aims at developing a simulation tool for discretely quantifying radiant distribution.

Although many studies have been conducted on thermal radiation simulation for arbitrary complicated geometries, few works address distribution of radiant contribution factor. An important characteristic is that visualized images of calculation results (such as surface temperature distribution) differ from measured thermal images (which closely approximate the radiation environment as seen from a human perspective by use of radiant temperature). By reproducing such measured mechanism, it is enabled to build an evaluation system with high accuracy (such as directivity of radiation) and high adaptability (such as the model of space, calculation position).

By focusing on the scheme for generating measured thermal images, this paper attempts to quantify distribution of radiant factor as the distribution of radiant temperature. In this process, we aim at two objectives:

1) Measured images and images obtained by a human eye are obtained by sensors of different shape. A method taking into account the shape of the human eye for radiant temperature is studied.

2) Anisotropic diffuse properties can be detected from infrared images of a glass surface. To reproduce these properties, we apply a shading calculation model used in generating computer graphics to the calculation of radiant temperature.

We then study the effect of surface properties and sensor shape on radiant temperature, by simulating radiant temperature by use of boundary conditions of actual data collected in a glass-enclosed space in Tokyo.

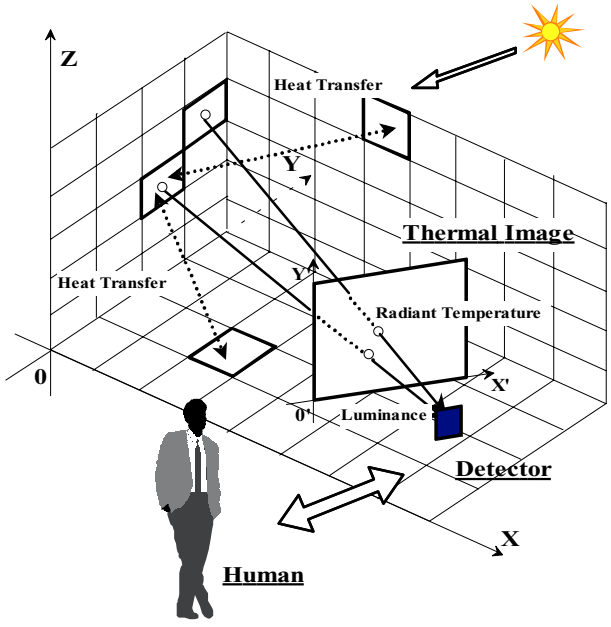

Fig. 1. Generating process of thermal image

IMAGE GENERATING PROCESS

Fig. 1 describes the method of generating thermal images. This process can be roughly divided into the following three processes.

1) Heat transfer between space elements (radiation, convection and conduction) that depends on outdoor conditions, three-dimensional figures, and material.

2) Derivation of luminance distribution from surface element to sensor.

3) Conversion of luminance intensity to radiant temperature.

This paper pertains to processes 2) and 3).

In computer graphics calculation, the human eye is modeled as a point sensor (or a small surface element), and luminance from a surface element to the sensor is calculated so as to derive rendered images. However, sensor shape is an important consideration in thermal images obtained from the human eye. Radiant temperature derived from measured thermal images and that derived from images captured by the human eye differ, because of differences in sensor shape.

Calculation of luminance intensity must be coupled with heat transfer calculation, but recalculation for changing viewpoint is not required. For a practicable system, heat exchange calculation results must be reiterated.

RADIANT TEMPERATURE

In order to calculate radiant temperature of a surface from luminance, we attempt to express radiant temperature as a function of luminance.

A thermal image photographed with a radiation detector can be thought of as an expression of radiant heat distribution from surfaces to the point of measurement. The information content of a photographic thermal image can be described as a translation of the temperature of black body radiation energy detected by the radiation detector. Now, radiant temperature $T_{R(j,i)}$ from a surface j to a dimensionless surface i is expressed as a function of luminance $L_{(j,i)}$ by Eq. 1.

$$T_{R(j,i)} = \sqrt[4]{\frac{\pi \cdot L_{(j,i)}}{\sigma}} \qquad (1)$$

In computer graphics, the human eye serving as a luminance sensor is modeled as a dimensionless surface, but the dimensional shape of the human eye serving as a radiant sensor must be considered in radiant heat transfer. When the human eye is modeled as consisting of dimensional surfaces: N_H, radiant heat quantity from a surface j to a human shape $Q_{H(j)}$ is expressed as a function of radiant temperature $T_{R(j,i)}$ by Eq. 2.

$$Q_{H(j)} = \sum_{i=1}^{N_H} A_{(i)} \cdot F_{(i,j)} \cdot \sigma \cdot T_{R(j,i)}{}^4 \qquad (2)$$

When radiant temperature from surface j to the human eye is defined as $T_{RH(j)}$, $Q_{H(j)}$ is expressed as a function of $T_{RH(j)}$ by Eq. 3.

$$Q_{H(j)} = A_H \cdot F_{H(j)} \cdot \sigma \cdot T_{RH(j)}{}^4 \qquad (3)$$

Consequently, $T_{RH(j)}$ is expressed by Eq. 4.

$$T_{RH(j)} = \sqrt[4]{\frac{\sum_{i=1}^{N_H} A_{(i)} \cdot F_{(i,j)} \cdot T_{R(j,i)}{}^4}{\sum_{i=1}^{N_H} A_{(i)} \cdot F_{(i,j)}}} \qquad (4)$$

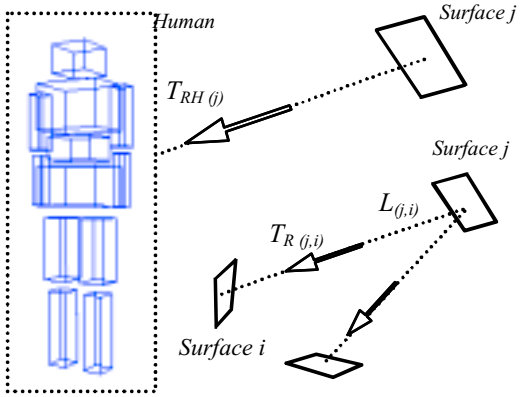

Fig. 2. Radiant temperature for human shape

ANISOTROPIC DIFFUSE PROPERTIES

Thermal Images of Glass Surface

Figs. 3(a) and 4(a) are measured infrared images of the surface of a glass wall of an atrium, taken from different angles. When these images are compared, reflectional radiation of opposed glass surface is shown clearly in Fig. 3(a), which is photographed in a direction perpendicular to the wall, but influence of reflectional radiation is different in Fig. 4(a), which is photographed from an oblique angle. Figs. 3(b) and 4(b) express numerical difference in radiant temperature distribution, in the form of an area histogram (enclosed by white lines).

Fig. 3(a). Infrared image parallel to window

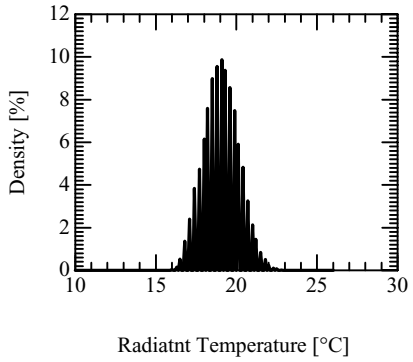

Fig. 3(b). Area histogram

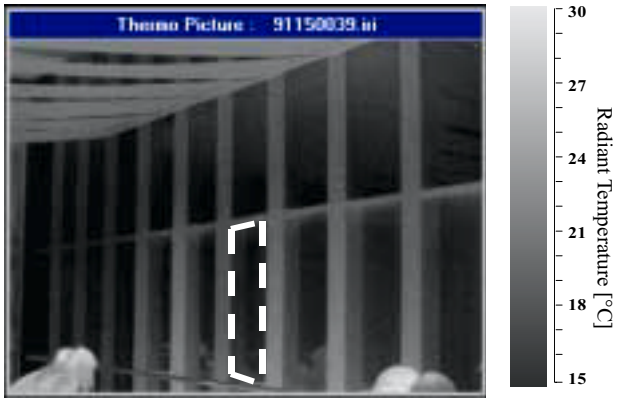

Fig. 4(a). Obliquely photographed infrared image

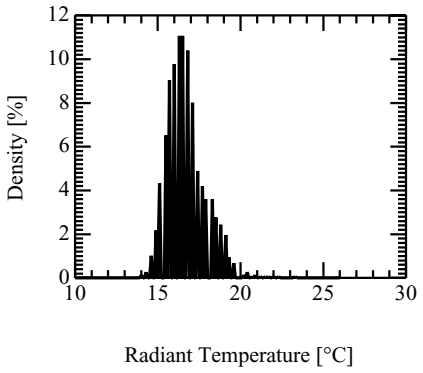

Fig. 4(b). Area histogram

This phenomenon is attributable to the anisotropic diffuse reflection properties of infrared radiation at a glass surface. Conceivably, such reflection properties affect calculation results of radiant environment distribution within the glass-enclosed space.

Shading Calculation Method

Methods of calculating reflectional luminance are generally based on ray tracing in computer graphic images. Calculations that take viewpoint into account are comparable to shading calculations used in generating computer graphics. However, methods for shading calculation are wide-ranging, and depend on considerations such as computation time and accuracy. If computation time is of primary concern (as in animation), shading calculations may involve simply ray tracing. However, if accuracy is the primary consideration, shading calculations must involve calculation of luminance distribution for different viewpoints. In this study, in order to attain greater accuracy, we applied shading calculation methods to calculations of radiant heat transfer.

Reflection Model

In order to accurately simulate radiant heat transfer, we employed the principles of shading calculation. Application of the principles employed in the study of luminosity can be helpful in the development of a detailed theoretical understanding of visible luminance behavior (such as BRDF). In this study we approached the modeling of thermal radiant reflection according to principles employed in the study of radiant intensity.

A surface's luminosity distribution of reflected radiation is assumed to follow the model depicted in Fig. 5. In this model, luminosity distribution consists of two elements. One element is isotropic diffuse reflection as per Lambert's law, which, regardless of incident angle, complies with the cosine law of reflectional angle. The other element is anisotropic diffuse reflection as per the Phong model, which complies with the cosine law (raised to the power of directional intensity value n) of the angle between the regular direction of incident angle θi and the reflectional angle θo. Radiant intensity of the

directional reflection element is expressed as a function of θh in Eq. 5.

$$i_r{}^b(\theta_h) = i_{rn}{}^b \cdot \cos^n \theta_h \qquad (5)$$

In this paper, this reflective model is simplified as follows. The regular rate of total reflectional energy is defined as $r(\theta i)$. In this regular rate, the rate of diffuse reflection is defined as the diffuse reflectance ρ^d, and the rate of bidirectional reflection is defined as the boundary reflectance ρ^b.

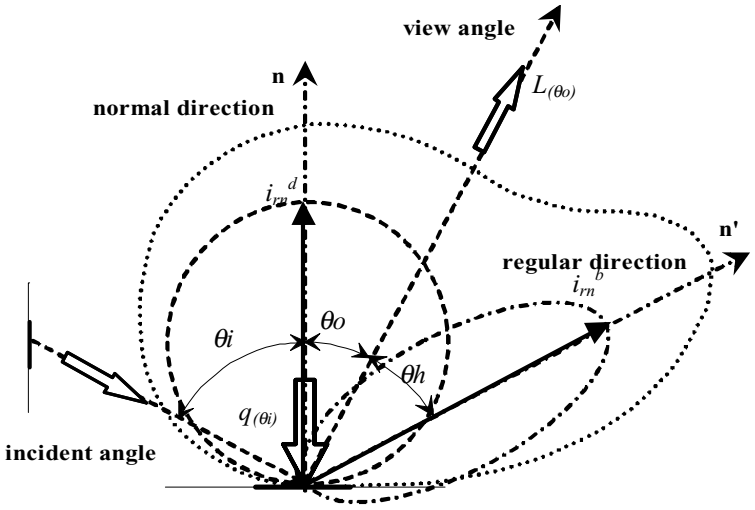

Fig. 5. Reflective luminosity model

The quantity of directional reflection heat at an incident angle θi is obtained by integrating reflectional intensity over the hemisphere, the regular direction of incident angle (Fig. 6).

$$Q_r{}^b(\theta_i) = \iint i_r{}^b(\theta_h) \cdot \sin\theta_h d\theta_h d\phi_h$$

$$= \iint i_{rn}{}^b \cdot \sin\theta_h \cdot \cos^n \theta_h d\theta_h d\phi_h$$

$$= \frac{2\pi}{n+1} \cdot i_{rn}{}^b \qquad (6)$$

In accordance with the relationship between regular reflectance and directional reflection properties, the equation for reflective luminance can be extended as follows.

$$L_{r(\theta i;\theta o)} = r_{(\theta i)} \cdot \left(\frac{\rho^d}{\pi} + \frac{n+1}{2\pi} \cdot \frac{\cos^n \theta_h}{\cos\theta_o} \cdot \rho^b \right) \cdot q_{(\theta i)} \qquad (7)$$

The example of calculation of BRDF is shown in Figs. 7 and 8

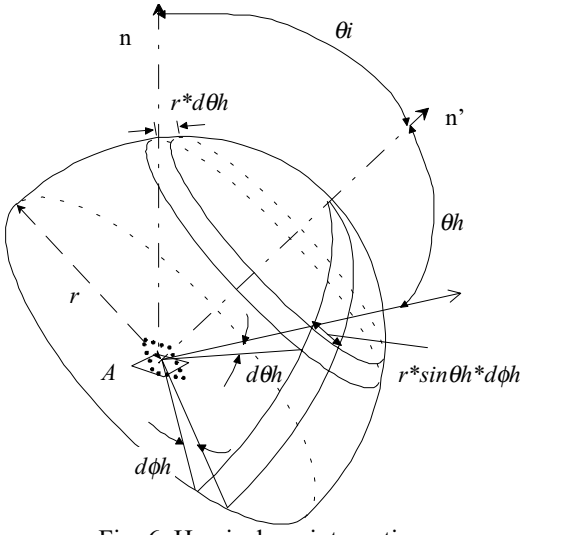

Fig. 6. Hemisphere integration

Discrete Calculation Method

When Eq. 7 is transformed discretely for calculation of luminance of finite closed surfaces, a discrete error arises in the boundary reflection component. Thus, with the application of modification coefficients, κ, surface luminance at reflectional angle θo, is calculated as follows (received radiant heat from surface j to i, $q_{(j,i)}$ [W/m^2], including interreflection, is assumed to be equal to the isotropic diffuse interreflection).

$$L_{r(j,i;i,\theta o)} = r_{(i,\theta i)} \sum_{j=1}^{N} \left(\frac{\rho^d{}_{(i)}}{\pi} + \rho^b{}_{(i)} \cdot \kappa_{(i)} \cdot \frac{n+1}{2\pi} \cdot \frac{\cos^n \theta_{h(i,j)}}{\cos\theta_{o(i)}} \right) \cdot q_{(j,i)} \qquad (8)$$

$$\kappa_{(i)} = 1 / \sum_{j=1}^{N} \frac{n+1}{2\pi} \cdot \frac{\cos^n \theta_{h(i,j)}}{\cos\theta_{o(i)}} \cdot F_{(i,j)} \qquad (9)$$

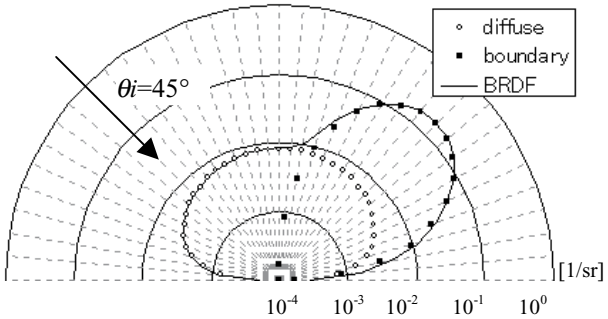

Fig. 7. BRDF (r=0.1, ρ^b=50%, ρ^d=50%, n=20)

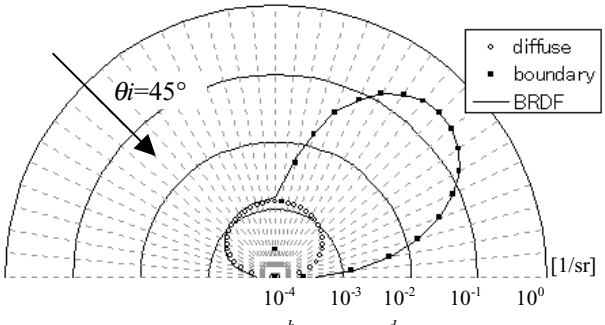

Fig. 8. BRDF (r=0.1, ρ^b=20%, ρ^d=80%, n=20)

Simulation of Radiant Temperature

Outline of Simulation

In order to account for effects of surface reflection, radiant temperature of the glass-enclosed space was determined through calculations that incorporate the principles discussed in the preceding sections.

An east-west section of the atrium is shown diagrammatically in Fig. 9. The ceiling and the east wall are glazed, and all other surfaces are unglazed. Divided mesh number is 310 and the human shape is modeled as a cube.

Table 1 shows surface temperature distribution of boundary conditions that based on actual measurement data of an atrium in Tokyo. Parameters of surface properties and viewpoint are represented as: A (diffuse / boundary reflection rate), B (directional intensity value), and C (view position) (Table 2 and Fig. 9). Also, all surfaces are assumed to have an emissivity of 0.9.

Effects of Reflection Properties

Simulation results are expressed as the difference between surface temperature and radiant temperature. Fig. 10 and Fig. 11 show surface temperature condition and difference of vertical distribution at east glazed wall in summer and winter. The difference is small in winter. So the results for summer conditions (Fig. 10) are discussed.

Under isotropic diffuse conditions, the difference in radiant temperature is relatively low at higher points on the wall that strongly depend on surface temperature distribution. Under anisotropic diffuse conditions, the temperature differences at mid-height increases with boundary reflectance that apparently differ from diffuse conditions.

Whereas total reflectance parameter equals 0.1, by the rate of bidirectional reflection ρ^b increasing, difference reach nearly 2°C (at ρ^b equal 100%, Fig. 10(a)). The difference is greatest at a height approximately halfway up the atrium walls. The same tendency was seen in directional intensity and it turns out that this is also an important factor (Fig. 10(b)). On the other hand, radiant temperature gradually increases as viewpoint approaches the surface of the glass wall (Fig. 10(c)). At that point, temperature difference in the same surface element reaches nearly 1°C as the viewpoint moves. Here, it turns out that the influence of a viewpoint is higher in the space lower part.

As mentioned above, by taking directional reflection into consideration, a significant difference of the radiant temperature at glazed wall was seen in the lower part from the center of wall where the form factor seen from a human body becomes larger.

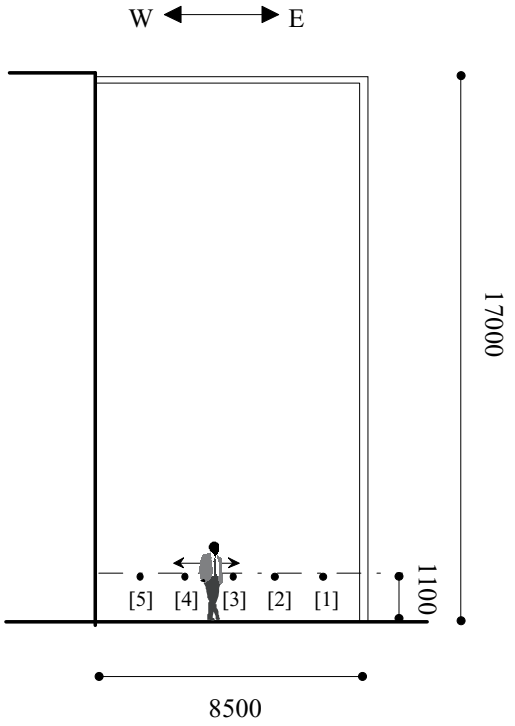

Fig. 9. Simulation model

Table 1. Boundary conditions of surface temperature

	Floor	Ceiling	Wall
Summer	30 °C	60 °C	Shown in Fig.8
Winter	15°C	25 °C	Shown in Fig.9

Table 2. Study items and parameters

	Study items	Fixed parameter
A	Reflectance	n = 100 View position = [3]
B	Directional intensity	(ρ^d,ρ^b) = (20% ,80%) View position = [3]
C	View position	(ρ^d,ρ^b) = (20% ,80%) n=100

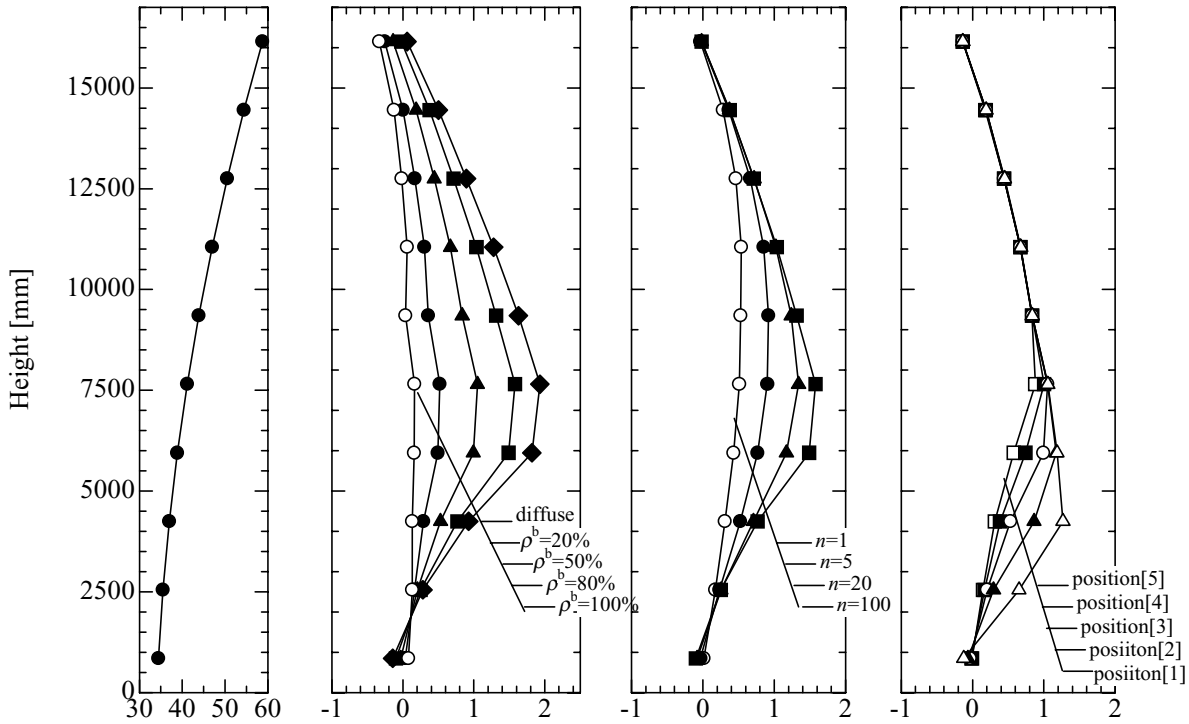

Fig. 10. Calculation results of summer condition

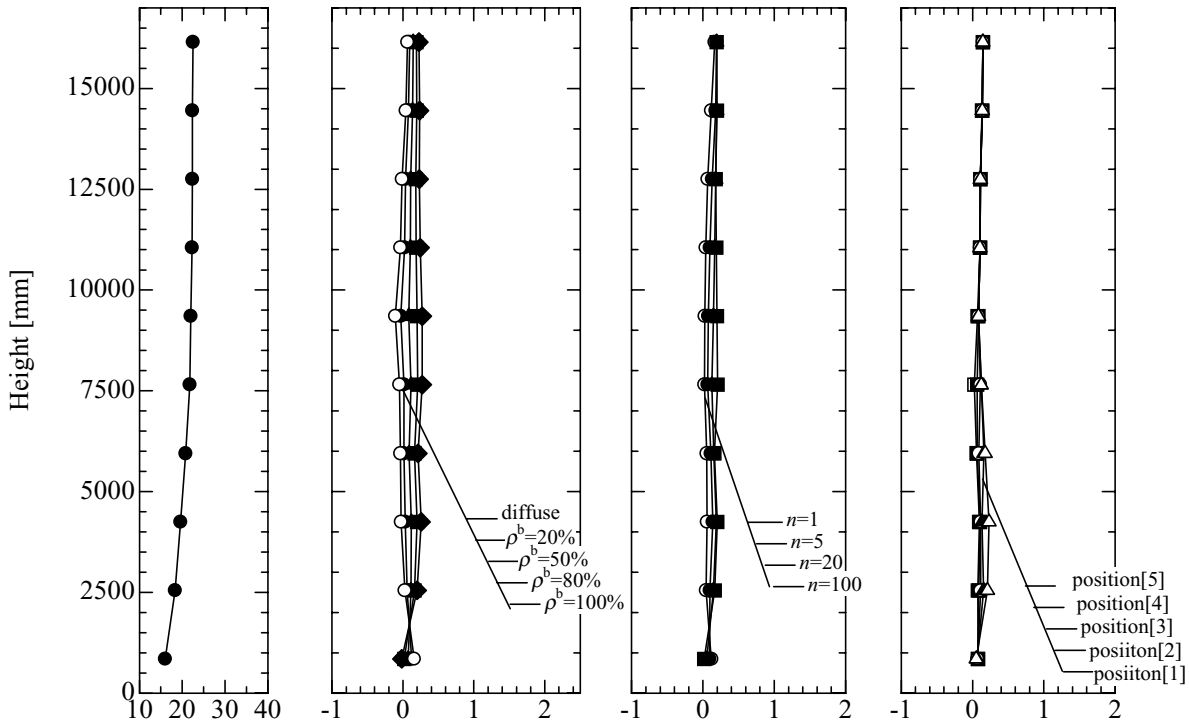

Fig. 11. Calculation results of winter condition

Effects of Human Shape

In the preceding section, human shape is modeled by a small cube. In this section, human shape is modeled by 12 cuboids, as shown in Fig. 12. Radiant temperature is calculated under standard summer conditions. Fig. 13 shows the radiant temperature differences for both the cubic model of the human eye used earlier and the model used here (each region), at the glass wall.

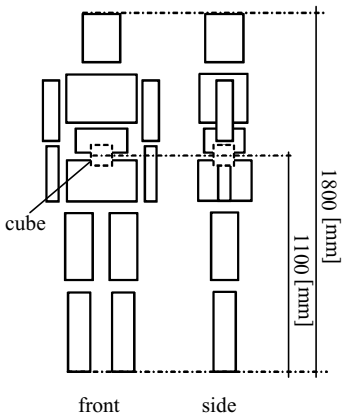

Fig. 12. Human shape

The overall difference for the model used here is greater than that for the cubic model, reaching nearly 0.5°C. In particular, differences between regions are greater at lower points, where form factor is high.

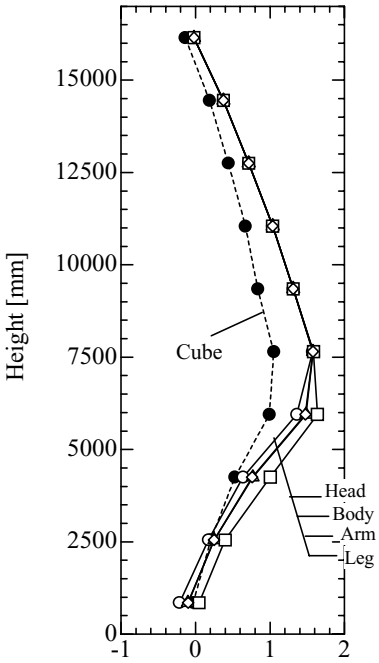

Fig. 13. Comparison of sensor shape

CONCLUSION

The method described in this paper can be used to predict radiant temperature distribution in an interior space involving anisotropic diffuse reflection, according to a detailed theoretical model. The results of a simulation conducted in an atrium clearly indicate that differences in radiant temperature are related to reflective properties of surfaces, position of the viewpoint and shapes of sensors. These can be concluded as follows.

1) The influence of directive reflection appears in a summer notably. On the other hand, in winter, it is minute.

2) When directional reflection is introduced in glass wall, a significant influence is shown greatly in central part from the space lower part. When regular rate of total reflectional energy $r(\theta i)$ is given 0.1 and the boundary reflectance ρ^b is changed 0% to 100%, difference between radiant temperature and surface temperature reach nearly 2°C at a height approximately halfway up the atrium walls.

3) The influence of the position of the viewpoint was greatly seen in the space lower part closer to the human body, and radiation temperature changes about 1°C to the same surface.

4) The overall difference for the cuboids model is greater than that for the cubic model, reaching nearly 0.5°C. In particular, differences between regions are greater at lower points.

REFERENCES

(1) K. Kohri, H. Ishino and T. Furukawa, “A Study on Evaluation of Radiant Effect from Each Surface in Atria Through Field Measurement”, Journal of Architecture, Planning and Environmental Engineering., Architectural Institute of Japan, No. 535, pp.9-14, 2000.9.

(2) M. Ichinose and H. Ishino, “A Study on Bidirectional Reflectance of Radiant Temperature in Glass Surface of Atrium Space”, Summaries of Technical Papers of Annual Meeting, Architectural Institute of Japan (D-2), pp.25-26, 2000.9.

(3) Y. Uetani and K. Matsuura, “A Method of Luminance Calculation in an Anisotropic Diffuse Reflecting Interior”, Journal of the Illuminating Engineering Society, pp.166-175, 1993.

(4) Y. Ashie, “A Survey on Radiant Intensity Distribution of The Short and Long Wave Zones Outdoors”, Journal of Architecture, Planning and Environmental Engineering., AIJ, No. 500 pp.71-77, 1997.1.

(5) William L. Wolfe and George J. Zissis, “The Infrared Handbook (revised edition)”, IRIA Series in Infrared & Electro-Optics, 1993.

NOMENCLATURE

σ = Stefan-Boltzmann constant
$A_{(i)}$ = Square of surface i [m^2]
$F_{(i,j)}$ = Form factor from surface i to j [-]
$T_{R(j,i)}$ = Radiant temperature of surface i from j [K][°C]
$L_{(j,i)}$ = Luminance from surface j to direction of i [W/(m^2*sr)]
$Q_{H(j)}$ = Received radiant heat quantity from surface j to human eye [W]
A_H = Square of human surface [m^2]
$F_{H(j)}$ = Form factor from human to surface j [-]
$T_{RH(j)}$ = Radiant temperature of surface j for human [K][°C]
N_H = Surface number of human eye shape [-]
N = Surface number of space [-]
$i_r{}^b{}_{(\theta)}$ = Boundary reflective luminosity [W/sr]
$i_{rn}{}^b$ = Boundary Reflective luminosity of normal direction [W/sr]
$Q_r{}^b$ = Radiant heat quantity of boundary reflection [W]
$L_{r(\theta i;\theta o)}$ = Reflective luminance [W/(m^2*sr)]
$r_{(i)}$ = Regular reflectance [-]
$\rho^d{}_{(i)}$ = Diffuse reflectance ratio[-]
$\rho^b{}_{(i)}$ = Boundary reflectance ratio[-]
θ_i = Incident angle [rad]
θ_o = View angle [rad]
θ_h = Angle between regular reflection and view direction [rad]
n = Directional intensity value [-]
$q_{(i)}$ = Received radiant heat from surface j to i [W/m^2]
$\kappa_{(i)}$ = Modification coefficients [-]